Metallic spherical anechoic chamber for antenna pattern measurement

Ali Farahbakhsh[†] and Mohammad Khalaj-Amirhosseini[‡]

The Electrical Engineering Department, Iran University of Science and Technology, Tehran, Iran

(Received 20 December 2015; revised manuscript received 21 April 2016; published online 25 June 2016)

Anechoic chambers are used for indoor antenna measurements. The common method of constructing an anechoic chamber is to cover all inside walls by the electromagnetic absorbers. In this paper, a fully metallic spherical chamber structure is presented in which the propagation of the electromagnetic waves inside the chamber is controlled and they are guided to an absorber. In the proposed method, an appropriate quiet zone is obtained, and unlike ordinary anechoic chambers, the absorber usage amount is reduced greatly. The performance of the chamber is evaluated by simulation. The results show that the proposed method could provide a useful technique for the indoor antenna measurements.

Keywords: absorber usage reduction, anechoic chamber, antenna measurements, metallic spherical chamber

PACS: 84.40.Ba, 84.40.–x, 41.20.Jb **DOI:** 10.1088/1674-1056/25/8/088401

1. Introduction

The need for indoor testing of antennas, which began in the early 1950s,[1] has led to anechoic chambers where the walls are covered by the electromagnetic (EM) absorbers to suppress the wall reflections, and thus obtaining a quiet zone. Building an anechoic chamber involves a significant financial investment. Some methods have been presented in the literature to optimize anechoic chambers to achieve better performance and lower cost.

A survey of the literature on anechoic chambers indicates that there are some conventional methods to minimize the absorber usage amount in anechoic chambers.[2–4] In Ref. [4], the ray-tracing method and genetic algorithm are used to optimize the layout of ferrite tile absorber in a partially lined rectangular enclosure to produce an acceptable quiet zone inside the chamber. By using this method, 20% of the chamber absorbers is reduced. In addition, a number of techniques have been presented to increase the performance of the anechoic chamber by changing the chamber shape.[5] Chamber shaping has some advantages such as propagation control of the electromagnetic waves to obtain optimum performance. Generally, there are three major types of anechoic chambers, i.e., rectangular,[5] tapered,[6] and double-horn[7,8] chambers. Although, the most used chamber for antenna measurement is of rectangular type, but they are not suited for VHF/UHF measurements due to the high reflection of absorbers at these frequencies. Instead of trying to surpass the absorber reflections, tapered and double-horn chambers are suggested to form a uniform illumination across the quiet zone by controlling the absorber reflection waves. Recently, a metallic ellipsoid anechoic chamber has been presented for reducing the absorber usage amount, which controls the EM wave propagation inside the chamber and guides them to an EM absorber.[9]

In this paper, a new anechoic chamber structure is presented by using a spherical chamber, the EM waves are guided to absorbers and therefore the number of electromagnetic absorbers are decreased is reduced greatly and a proper quiet zone is formed for the antenna measurement.

Reduction of absorber usage amount has some great benefits. Since a few absorbers are used, the absorbers can be easily changed for different frequency bands and therefore, wide band anechoic chamber is achieved by using the optimum absorber for each of the frequency bands. Also, it is desirable to test antennas in clean room conditions, that is hard to do in an anechoic chamber since classical carbon based foam absorbers tend to pollute the air. But the clean room condition in the spherical chamber is achievable because the absorbers on the chamber walls are omitted. The size of the spherical chamber is smaller than that in Ref. [9] and the spherical chamber needs less absorbers than the ellipsoid chamber. Also, the main benefit of the spherical chamber is that the scattering waves from the antenna under test (AUT) are guided to the absorber, that leads to a reliable measurement.

The rest of this paper is organized as follows. In Section 2 the design procedure of the new spherical chamber is presented. In Section 3, the VSWR method is presented to evaluate the quiet zone performance. A spherical chamber is designed and verified in Section 4. The effects of some mechanical imperfections and the AUT scattering on the quiet zone performance are investigated in Sections 5 and 6. Finally, conclusions are provided in Section 7.

[†] Corresponding author. E-mail: a_farahbakhsh@iust.ac.ir

[‡] E-mail: khalaja@iust.ac.ir

© 2016 Chinese Physical Society and IOP Publishing Ltd

2. Design of the spherical chamber

It can be shown by geometrical optics[10] that if a point source is placed on the surface of a metallic sphere, the rays are focused at a line on the opposite side of the sphere after reflection from the metallic surface as shown in Fig. 1. By placing an EM absorber material at the focus line, all EM rays are absorbed and consequently a quiet zone is formed inside the sphere as shown in Fig. 1.

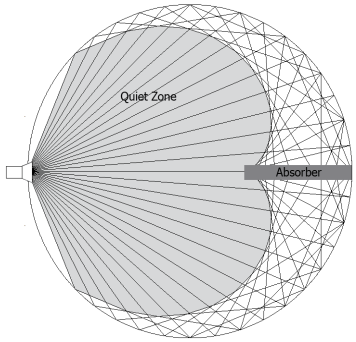


Fig. 1. Cross section of the spherical chamber.

Like ordinary anechoic chambers, a horn antenna is selected as the source antenna and it must be placed near the surface of the spherical chamber.[11]

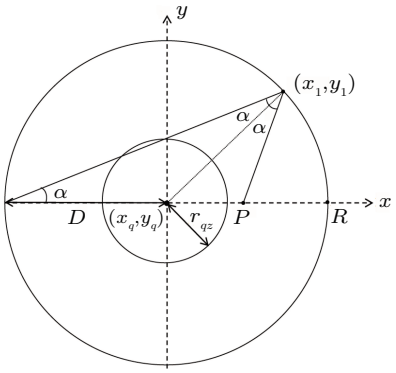


Fig. 2. General structure of the spherical chamber.

According to the definition, a quiet zone is a volume inside the chamber, which only contains one wave front from the source antenna. The level of reflected waves from surrounding objects within the quiet zone determines the performance of the anechoic chamber. Usually, the quiet zone is considered as a spherical volume.

The design procedure of the spherical chamber is to calculate the chamber radius by knowing the measuring distance (d) and the quiet zone radius (r_{qz}). According to Fig. 2, the EM rays cross the x axis at point P after reflection from the sphere surface. The position of P is dependent on the radiation angle of the ray (α). The quiet zone boundary is determined by the minimum value of P. By using some simple geometric relations, the position of P will be obtained.

$$x_1 = R\cos(2\alpha), \tag{1}$$

$$y_1 = R\sin(2\alpha). \tag{2}$$

And the position of P is

$$P = x_1 - y_1\tan(\pi/2 - 3\alpha). \tag{3}$$

Substituting expressions (1) and (2) in expression (3) and making some simplifications we have

$$P = \frac{R}{2\cos(2\alpha)+1}. \tag{4}$$

The minimum value of P is $R/3$. Therefore, the designing equation of the spherical chamber is given below.

$$R = 3\frac{d + r_{qz}}{4}. \tag{5}$$

The length of the absorber should be

$$L_{ab} = \frac{2R}{3}. \tag{6}$$

We need a cylindrical absorber inside the chamber. Only one piece on the absorber is used inside the chamber, so the absorber can be easily changed for different frequency bands and can be made of high performance and expensive material. In this paper, the absorber is made by putting some ordinary pyramid absorbers around a metallic cylinder as shown in Fig. 3.

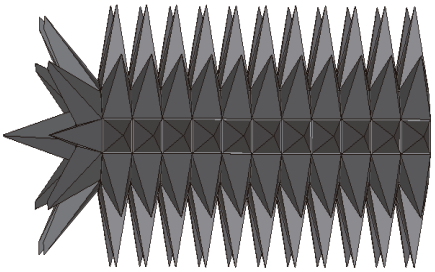


Fig. 3. Cylindrical absorber.

The position of AUT is important. If it is placed on the negative part of the x axis, the AUT scattered waves are converged on the absorber as shown in Fig. 4 and therefore the scattering of the AUT does not disturb the measurement.

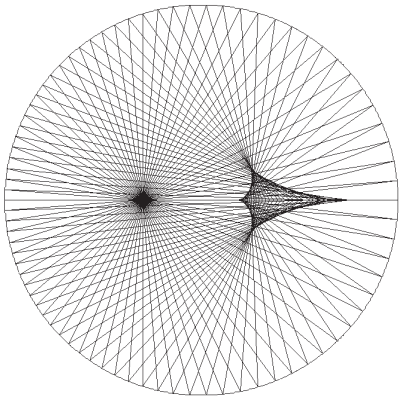


Fig. 4. AUT scattered EM waves focused on the absorber position inside the chamber.

3. Quiet zone performance

In this section, we illustrate the procedure of evaluation of the quiet zone performance inside the chamber. Here, this is done by measuring the electric field inside the quiet zone and calculating the voltage standing wave ratio (VSWR) of the electric field.[12,13] In practical measurements, a probe is explored inside the quiet zone and its output voltage is used for VSWR calculation. Clearly, the probe output voltage and the chamber electric field are directly proportional, and so VSWR could be obtained by using the electric field of the quiet zone.

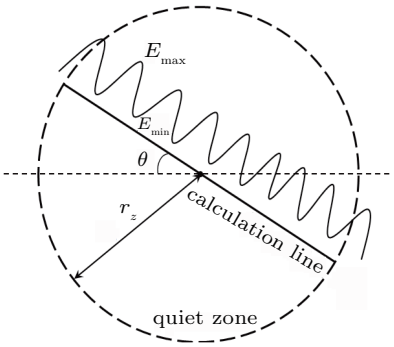


Fig. 5. Reflectivity is calculated on a straight line inside the quiet zone by finding the minimum and maximum of the electric field.

As shown in Fig. 5, by considering the local minimum ($E_{\min}$) and maximum ($E_{\max}$) amplitude of the electric field inside the quiet zone on a straight line (calculation line), VSWR can be calculated from[12]

$$\mathrm{VSWR} = \frac{E_{\max}}{E_{\min}}. \tag{7}$$

Then, the reflectivity level could be defined as[12]

$$\Gamma = 20\log\frac{\mathrm{VSWR}-1}{\mathrm{VSWR}+1}. \tag{8}$$

It is clear that the high value of the reflectivity shows the existence of reflected waves in the quiet zone. So, with a proper chamber for antenna measurements, the reflectivity level should be smaller than the standard value. Since the source of the reflections is unknown, in order to ensure the optimum performance of the chamber, the reflectivity levels in all directions should be considered. To do this, the VSWR calculation line is rotated inside the quiet zone and the maximum reflectivity level is computed.

4. Design example

In this section, a typical design is provided to illustrate the applicability of the proposed spherical chamber. In this numerical example, COMSOL[14] is used for full-wave simulations.

As an example, the operating frequency is assumed to be 1 GHz–20 GHz and therefore the maximum operating wavelength is 30 cm. The quiet zone radius is assumed to be 50 cm and the measuring distance (d) to be 1 m. Then the radius of the chamber is obtained by using expression (4) as

$$R = 3\frac{d + r_{qz}}{4} = 1.125 \text{ m}, \tag{9}$$

and the absorber length should be

$$L_{\mathrm{ab}} = \frac{2R}{3} = 75 \text{ cm}. \tag{10}$$

To ensure that the antenna under test (AUT) is located in the far-field of the source antenna, the following constrain should be satisfied:

$$d > \frac{2D_{\max}^2}{\lambda}, \tag{11}$$

where D_{max} is the largest dimension of AUT and should be

$$\text{at 1 GHz, } \lambda = 0.3 \text{ m}, D_{\max} < \sqrt{\frac{d\lambda}{2}} = 39 \text{ cm}, \tag{12}$$

$$\text{at 20 GHz, } \lambda = 0.015 \text{ m}, D_{\max} < \sqrt{\frac{d\lambda}{2}} = 8.7 \text{ cm}. \tag{13}$$

In order to ensure the acceptable performance of the designed chamber, numerical simulations are performed using COMSOL software which uses a finite element method to determine the electric field distribution inside the chamber. The electric field distributions at frequencies 2 GHz and 4 GHz inside the chamber are shown in Fig. 6. Also, the reflectivity level inside the quiet zone is calculated using the VSWR method in all of the directions and the maximum reflectivity level versus frequency is shown in Fig. 7.

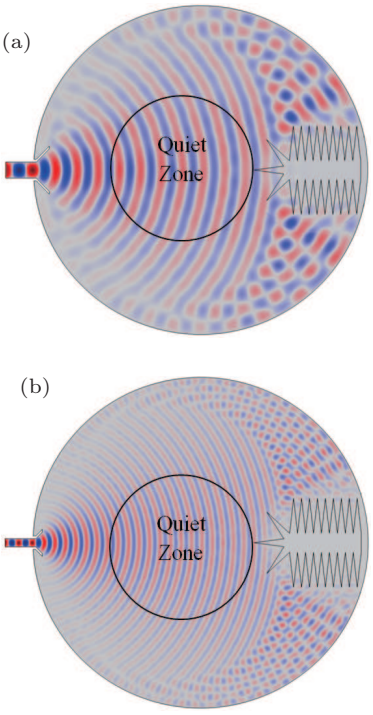


Fig. 6. (color online) Electric field inside the chamber at (a) 2 GHz and (b) 4 GHz.

The reflectivity level of a rectangular chamber[15] is also plotted in Fig. 7 for comparison. From this figure it follows

that as expected, by increasing the frequency, ray behavior of the EM wave becomes more visible and consequently the reflectivity level is reduced. From these results, one can find that the spherical chamber works well in the desired frequency range.

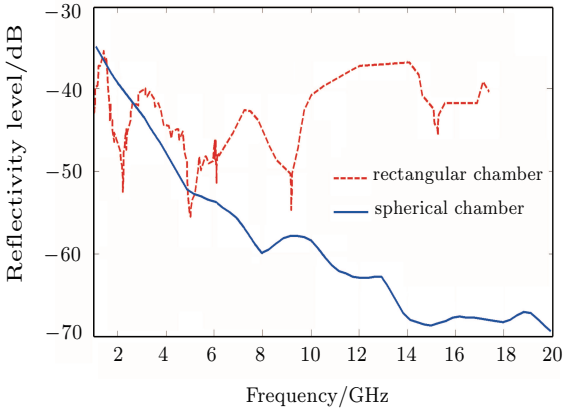


Fig. 7. (color online) Maximum reflectivity levels inside the quiet zone versus the operating frequency.

5. Mechanical imperfections

In the spherical chamber fabricating process, the mechanical accuracy specifies the fabrication cost; a more accurate process leads to a more expensive chamber. Hence it becomes necessary to study the effects of different distortions on the performance of the chamber.

In this section, we deal with the effects of surface roughness and shape deformation of the chamber in its reflectivity level and performance. Here, this is done by considering a small extent of distortion in the shape of the spherical chamber surface in polar coordinate, i.e.,

$$r_{\text{distorted}} = R + \frac{\Delta}{2}\sin\left(\frac{N\theta}{2}\right), \tag{14}$$

where r is the mathematical equation of the spherical chamber in polar coordinate with distortion, and N and Δ are the arbitrary parameters determining the distortion extent. Notice that with adjusting these two parameters, we can add arbitrary extent of distortion in roughness and shape of the chamber. In other words, the shape deformation and surface roughness are represented by large values and small values of N, respectively.

As an example, the reflectivity levels inside the quiet zone at 4 GHz for different values of Δ and N are calculated and the results are illustrated in Fig. 8.

Although the chamber performance is disturbed by increasing the distortion amplitude, even for 8-mm surface roughness and 9-cm shape deformation, this effect is not very critical and the reflectivity level remains lower than −20 dB. Therefore, one can conclude that the fabrication tolerance will not have a critical influence on the performance of the spherical chamber and especially the quiet zone.

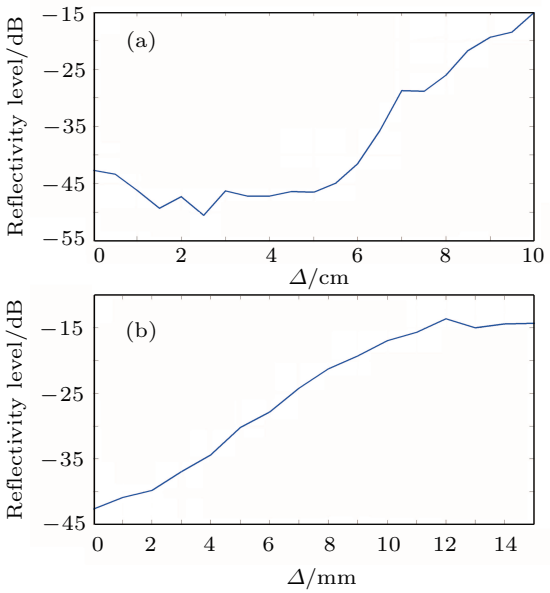


Fig. 8. (color online) Effects of (a) the chamber shape deformation ($N = 3$) and (b) the chamber surface roughness ($N = 100$) on the quiet zone reflectivity level.

6. AUT radiation pattern measurement

In this section, a standard 10-GHz horn antenna is used as the AUT.[16] The horn antenna is placed inside the quiet zone and its radiation pattern is measured by simulation.

The aperture dimension of the AUT is 3.5×2.6 cm and the AUT length is 4.5 cm. The normalized radiation pattern in the E-plane is obtained, which is plotted in Fig. 9.

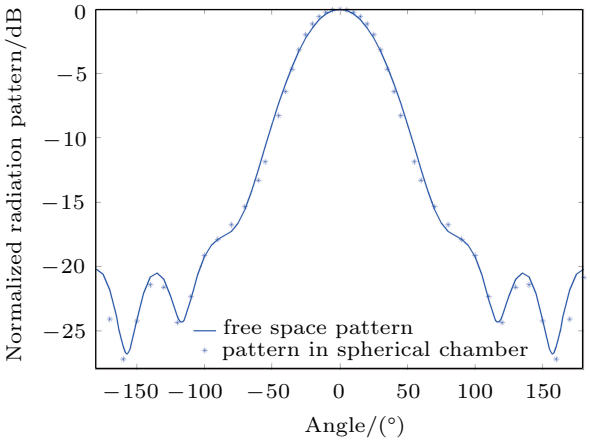


Fig. 9. (color online) Normalized radiation patterns of a standard horn antenna inside the spherical chamber and in free space.

As shown in Fig. 9, there is good agreement between the measured pattern inside the spherical chamber and the free space pattern.

7. Conclusions

In this paper we present a new metallic spherical anechoic chamber structure. By using the proposed structure, a quiet zone is obtained while the EM absorber usage amount is reduced greatly. Some numerical examples are given to validate

and test the performance of the proposed structure. The reflectivity level is calculated by the VSWR method inside the quiet zone, and the result indicates that the spherical chamber works well in the desired operating frequency band. Further, the effects of the chamber mechanical imperfections, i.e., shape deformation and surface roughness, on the quiet zone reflectivity level are investigated. The results show that these imperfections do not have critical and considerable destructive effects on the chamber, and the spherical chamber could be manufactured by cheap technologies. In addition, the pattern of a horn antenna is obtained in the spherical chamber by simulation and from the results, one can find that the spherical chamber has an acceptable performance.

References

[1] Emerson W H 1973 *IEEE Trans. Anten. Propag.* **21**, No. 4

[2] Kineros C and Ungvic V H 2003 *IEEE International Symposium on Electromagnetic Compatibility*, USA

[3] Bornkessel C and Wiesbeck W 1996 *IEEE Trans. Electromagn. Compat.* **38** 499

[4] Razavi S M J and Khalaj-Amirhosseini M 2008 *Prog. Electromagnet. Res. B* **9** 53

[5] Leland H Hemming 2002 *Electromagnetic Anechoic Chambers: A Fundamental Design and Specification Guide* (IEEE Press)

[6] Emerson W H 1967 USA Patent No. 3 308 463, March 1967, Anechoic Chamber

[7] Hemming L H 1985 USA Patent No. 4 507 660, March 26, 1985, Anechoic Chamber

[8] Sanchez G A 1997 USA Patent No. 5 631 661, May 20, 1997, Geometrically Optimized Anechoic Chamber

[9] Farahbakhsh A and Khalaj-Amirhosseini M 2015 *IEEE Trans. Anten. Propag.* **63** No. 9

[10] Islam T M 1994 *An Indoor Model of Electromagnetic Wave Propagation Using Ray Tracing* (Washington: University of Washington)

[11] Evans E G 1990 *Antenna Measurement Techniques* (London: Artech House)

[12] Togawa H, Hatakeyama K and Yamauchi K *IEEE Trans. Electromagn. Compat.* **47** 312

[13] Appel-Hansen J 1973 *IEEE Trans. Anten. Propag.* **AP-21** 490

[14] COMSOL Multiphysics® Modeling Software, 2014

[15] Anechoic chamber specification, Center of Remote Sensing of Ice Sheets, the University of Kansas

[16] WR-75 Standard Gain Horn Antenna Operates from 10 GHz to 15 GHz with a Normal 10-dB Gain SMA Female Input Connector, Pasternack, Technical Data Sheet, 2013